

Electronic Supplementary Information

ESI1. Freeze-evacuation process

To obtain O 1s spectra without any interference, 0.1 M HF electrolyte solution was employed, because HF contains neither oxygen nor a specifically adsorbing anion. Each test electrode was polarized at a given potential for 5 min in N₂-purged solution. Then, the electrode was emersed from the solution under potential control and promptly transferred to a UHV chamber evacuated by a sorption pump, and subsequently by a cryo-pump. The electrode surface was spontaneously cooled to a temperature below 220K, due to the latent heat of evaporation of the electrolyte droplet remaining on the electrode surface during the transfer to UHV (freeze-evacuation).¹ Figure E1 shows the temperature change of a Pt(111) single-crystal electrode (diameter 10 mm; thickness 0.5 mm) during the evacuation process, measured by an attached thermocouple. The temperature of the test electrode was found to decrease in two steps. In the first step, the electrode was cooled down to ca. 250 K following evaporation of the electrolyte droplet. At the same time, the electrolyte droplet was frozen on the electrode surface. In the next step, the electrode was further cooled down by sublimation of the frozen electrolyte on the surface in vacuum. At such low temperatures, bilayer water molecules can partially remain on the Pt surface, even in UHV, whereas the bulk water must be completely desorbed during the evacuation process.

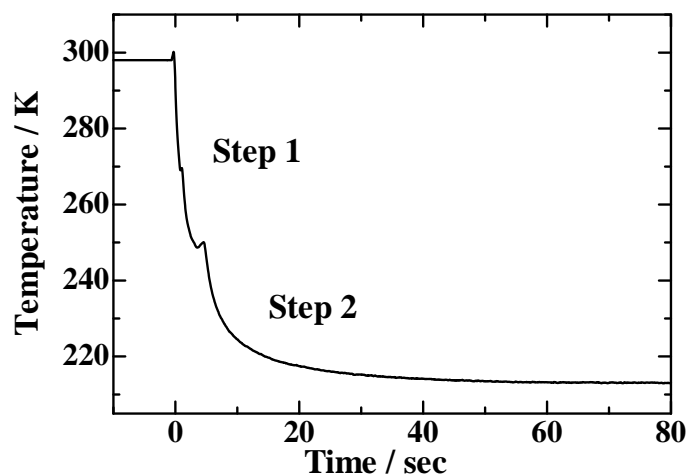


Figure E1. Temperature change of a Pt(111) single-crystal electrode during the evacuation process, measured by an attached thermocouple (chromel-alumel).

ESI2. Deconvolution of O 1s spectra

We deconvoluted the O 1s spectra into several asymmetric Lorentzian–Gaussian peaks with a linear background. Peak parameters such as full width at half-maximum (fwhm), tail scale (TS) and ratio of Gaussian to Lorentzian (G/L) were referred to those for a submonolayer of atomic oxygen (O_{ad}) formed on the polycrystalline Pt surface by O_2 exposure in vacuum.² The curve-fittings were performed for all spectra with the fwhm, TS and G/L parameters fixed as constants while allowing the peak energies and areas to vary.² Figure E2 shows typical results of the deconvolution of the O 1s spectra for the (a) Pt(111), (b) Pt(100) and Pt(110) electrodes after emersion from 0.1 M HF solution saturated with N_2 . All of the spectra were satisfactorily deconvoluted into the same components, even though the shapes of the spectra were quite different from each other, as shown in Figure E2.

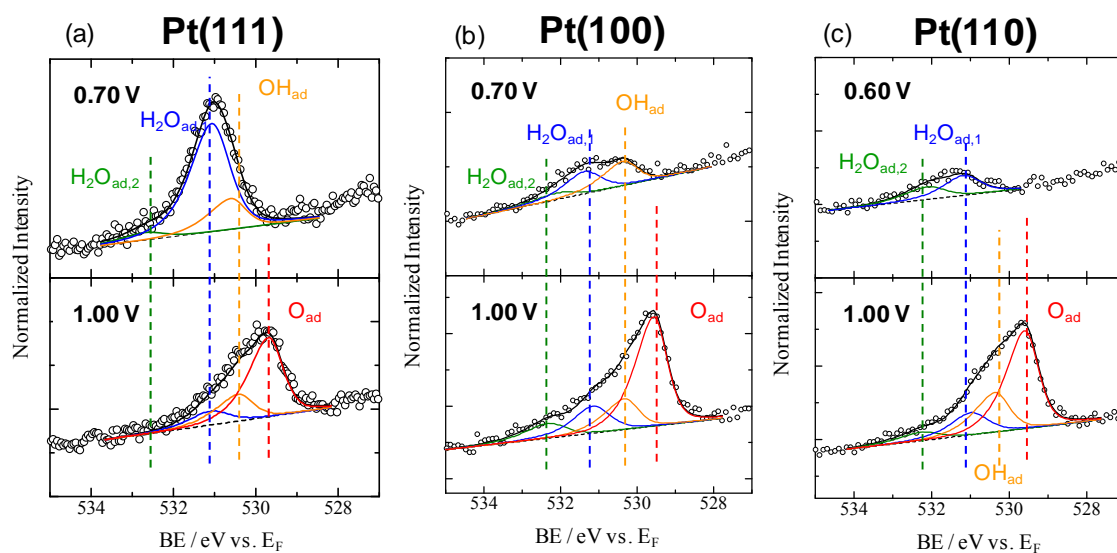


Figure E2. Deconvolution of O 1s spectra for the three single-crystal electrodes after emersion from 0.1 M HF solution saturated with N_2 : (a) Pt(111) at 0.70 and 1.00 V; (b) Pt(100) at 0.70 and 1.00 V; (c) Pt(110) at 0.60 and 1.00 V. Open circles and colored lines indicate experimental data and deconvoluted components, respectively. Dashed and black lines show the linear backgrounds and the resulting peaks of the composites, respectively.

ESI3. Monolayer matrix factor for each single-crystal electrode

Fractional coverages θ of oxygen species (atomic ratio of oxygen in the species to Pt) were calculated on the basis of the photoelectron intensities of deconvoluted O 1s and Pt 4f. Because the photoelectron intensity of the metal substrate (Pt 4f, kinetic energy =1400 eV) was only slightly attenuated by the submonolayer of each oxygen species, the following simple relation can be utilized:^{2,3}

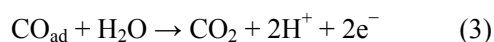
$$\theta = M_{O/Pt} I_O / I_{Pt} \quad (1)$$

where $M_{O/Pt}$, I_O and I_{Pt} are a monolayer matrix factor, and the photoelectron intensities of O 1s and Pt 4f, respectively. $M_{O/Pt}$ values for each single-crystal electrode were obtained on the basis of a relation between the coverage of a CO adlayer on the corresponding crystal electrode and the photoelectron intensity ratio of Pt 4f and O 1s for the CO adlayer via the following equation:

$$M_{O/Pt} = \theta_{CO} I_{Pt} / I_O \quad (2)$$

The CO adsorption was carried out in a CO-saturated 0.1 M HF solution for 0.1 V for 3 min. XP spectra of O 1s and Pt 4f for the CO adlayer were obtained after the CO adsorption. Figure E3a shows O 1s spectra normalized by the Pt 4f photoelectron intensities for the three single-crystal electrodes. For the Pt(111) and Pt(100) electrodes, the O 1s spectra were found to split due to different adsorption sites of CO. The BE components at 533 and 531 eV are attributed to bridge and on-top sites of adsorbed CO molecules, respectively.

The actual CO coverage at each crystal electrode was evaluated by the CO oxidation charge density Q_{CO} obtained in a stripping voltammogram in the 0.1 M HF solution purged with N_2 via reaction 3, by use of equation 4:



$$\theta_{CO} = Q_{CO} / (2 F \Gamma_{Pt}) \quad (4)$$

where F and Γ_{Pt} are the Faraday constant and the molar Pt surface density of each single-crystal electrode. Figures E3b-d show the stripping voltammograms at the three single-crystal electrodes after the corresponding XPS measurements. The $M_{O/Pt}$ values obtained are presented in Table 1. The values differed among the crystal planes due to the differences in the atomic densities of surface Pt and the elastic and/or inelastic scattering factors of the emitted Pt 4f photoelectrons.

Table 1. $M_{O/Pt}$ values for each single-crystal employed in the present study

	Pt(111)	Pt(100)	Pt(110)
$M_{O/Pt}$	20.6	30.4	32.9

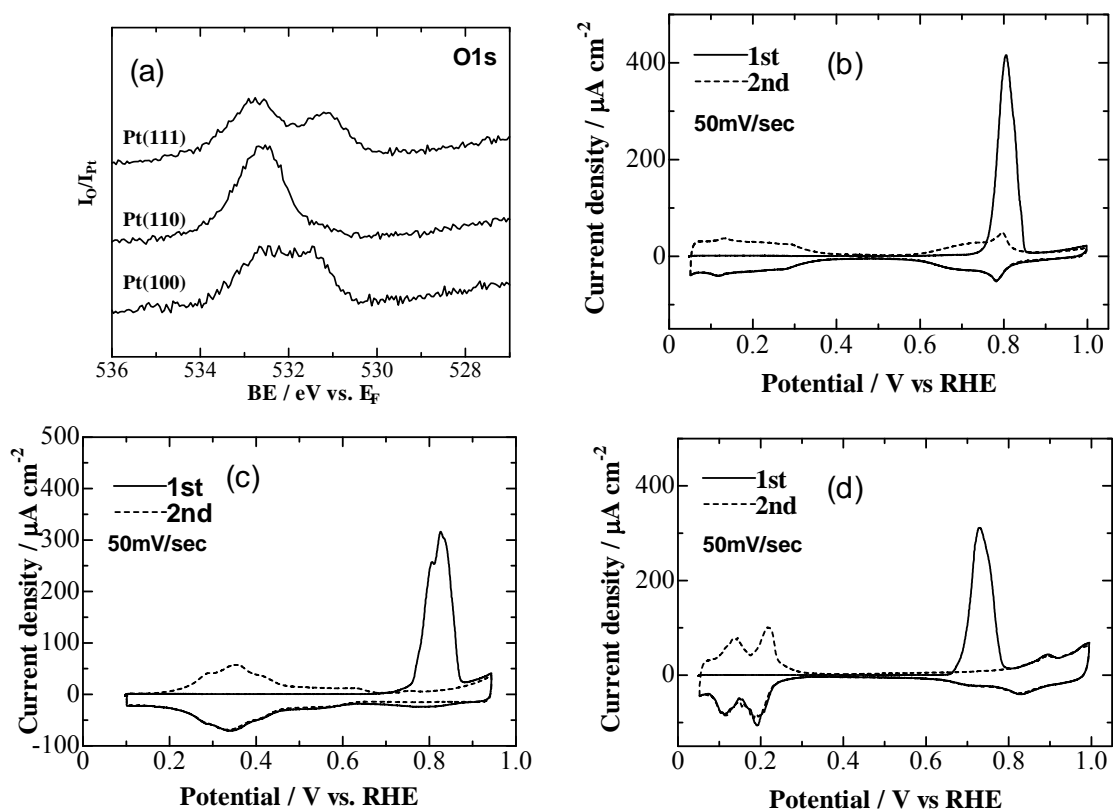


Figure E3. (a) O 1s spectra for CO adlayers on the three single-crystal electrodes after CO adsorption for 5 min in 0.1 M HF solution saturated with CO. CO-stripping voltammograms at (b) Pt(111), (c) Pt(100) and (d) Pt(110) electrodes in N₂-purged 0.1 M HF solution after the corresponding XPS measurements.

ESI4. Proposed models for the bilayer structures on the Pt single-crystal electrodes

It has been well established that water molecules form an ice-like bilayer structure on the Pt(111) surface at low temperatures in ultrahigh vacuum.⁴ Ogasawara et al. have analyzed this bilayer structure by using XPS and evaluated the distance between the two water layers from the O 1s BE splitting, on the basis of a final-state hole-screening theory.⁵ The theory explains the lower O 1s BE of the first-layer water molecule and predicts a short distance between the molecule and the Pt surface due to the image charge.⁵ Thus, the $\text{H}_2\text{O}_{\text{ad}}$ observed at 531.1 eV in the present study can be assigned to the first-layer water, which is bound directly to the Pt surface through an O lone pair, while the feature at 532.7 eV can be assigned to the second-layer water, which interacts with the first layer via hydrogen bonding.⁶ The proposed bilayer model is illustrated in Figure E4a. According to this model, the theoretical coverage of $\text{H}_2\text{O}_{\text{ad}}$ is 0.67 at Pt(111). At $E = 0.8$ V, the sum of $\theta[\text{OH}_{\text{ad}}]$ and $\theta[\text{H}_2\text{O}_{\text{ad},1}]$ became nearly equal on Pt(111), and the sum of these coverages reached a maximum of 0.68, coinciding, within experimental error, with the theoretical coverage of bilayer water molecules. This agreement suggests that the honeycomb framework of the bilayer remained during the initial surface oxidation process at Pt(111). A structural model for the mixed $\text{OH}_{\text{ad}}/\text{H}_2\text{O}_{\text{ad},1}$ layer at 0.8 V is illustrated in Figure E4b. This structure, with $\theta[\text{OH}_{\text{ad}}] = \theta[\text{H}_2\text{O}_{\text{ad},1}]$, should be the most stable among the possible $\text{OH}_{\text{ad}}/\text{H}_2\text{O}_{\text{ad},1}$ layers, because the hydrogen bonding network (HBN) is complete, as reported in a theoretical study.⁷

In contrast to Pt(111), the Pt(100) electrode surface exhibited no increment of $\theta[\text{H}_2\text{O}_{\text{ad},1}]$ even though $\theta[\text{OH}_{\text{ad}}]$ increased. This is because the HBN honeycomb structure might be unstable on the Pt(100)-(1 × 1) surface due to a mismatch between the honeycomb layer of the oxygen species and the rectangular surface geometry. If the bilayer forms on the Pt(100) surface with retention of the HBN framework, the adsorption sites of the water molecules cannot be determined (incommensurate), as shown in Figure E4c.

On the Pt(110) surface, it has been reported by Fusy et al. in their study⁸ by using electron-stimulated desorption ion angular desorption that water molecules can form the bilayer structure at 100K in UHV. On the basis of that study, a model can be proposed for the bilayer formed on Pt(110) in 0.1 M HF solution, as presented in Figure E4d. In this model, one thirds of the adsorbed water molecules are located at the top sites on ridges, while the rest are located near the top sites on the second Pt layer.

References

- (1) M. Wakisaka, H. Uchida and M. Watanabe, in *Fuel Cell Science: Theory, Fundamentals, and Biocatalysis*, ed. A. Wieckowski and J. K. Nørskov, Wiley, New Jersey, 2010, ch. 4, pp.147-168.
- (2) M. Wakisaka, H. Suzuki, S. Mitsui, H. Uchida and M. Watanabe, *J. Phys. Chem. C*, 2008, **112**, 2750.
- (3) D. Briggs and M. P. Seah, Eds., *Practical Surface Analysis, 2nd ed.; Volume 1: Auger and*

X-ray Photoelectron Spectroscopy, 1990, Wiley, New York.

(4) M. A. Henderson, *Surf. Sci. Rep.*, 2002, **46**, 1.

(5) H. Ogasawara, B. Brena, D. Nordlund, M. Nyberg, A. Pelmenschikov, L. G. M. Pettersson and A. Nilsson, *Phys. Rev. Lett.*, 2002, **89**, 276102.

(6) M. Wakisaka, H. Suzuki, S. Mitsui, H. Uchida and M. Watanabe, *Langmuir*, 2009, **35**, 1897.

(7) C. Clay, S. Haq, A. Hodgson, *Phys. Rev. Lett.*, 2004, **92**, 046102.

(8) J. Fusy and R. Ducros, *Surf. Sci.*, 1990, **237**, 53.

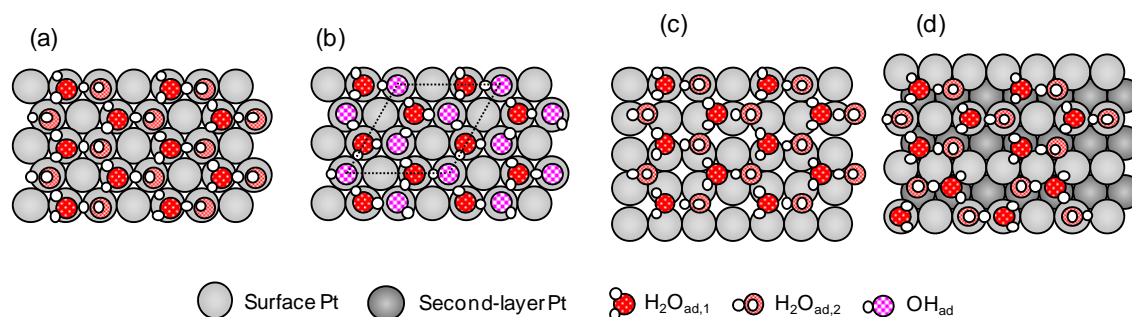


Figure E4. Proposed structural models for (a) the bilayer water on Pt(111), (b) the mixed $\text{OH}_{\text{ad}}/\text{H}_2\text{O}_{\text{ad},1}$ layer with the strong hydrogen-bonding network on Pt(111), (c) an unstable, incommensurate water bilayer on Pt(100), and (d) a commensurate water bilayer on Pt(110).